

# Terrestrial Planets Formation under Migration: the Systems near 4:2:1 Mean Motion Resonance

Zhao Sun<sup>1,2</sup>, Jianghui Ji<sup>1\*</sup>, Su Wang<sup>1</sup>, Sheng Jin<sup>1</sup>

<sup>1</sup>CAS Key Laboratory of Planetary Sciences, Purple Mountain Observatory, Chinese Academy of Sciences, Nanjing 210008, China

<sup>2</sup>University of Chinese Academy of Sciences, Beijing 100049, China

Accepted. Received; in original form

## ABSTRACT

In this work, we extensively investigate the formation of near 4:2:1 mean motion resonances (MMRs) configuration by performing two sets of N-body simulations. We model the eccentricity damping, gas drag, type I and type II planetary migration of planetesimals, planetary embryos and giant planets in the first sets. For the simulations of giant planets with type II migration, the massive terrestrial planets, with a mass up to several Earth masses, are likely produced in the systems. We further show that by shepherding and/or scattering mechanisms through Jovian planet's type II migration, the terrestrial planets and giant planets in the systems can be evolved into a near 4:2:1 MMRs. Moreover, the models are applicable to the formation of Kepler-238 and 302 systems. In the second set, we study the 4:2:1 MMRs formation in the terrestrial planetary systems, where the planets undergo type I migration and eccentricity damping. By considering type I migration,  $\sim 17.1\%$  of the simulations indicate that terrestrial planets are evolved into 4:2:1 MMRs. However, this probability should depend on the initial conditions of planets. Hence, we conclude that both type I and type II migration can play a crucial role in close-in terrestrial planet formation.

**Key words:** planetary systems – methods: numerical – planets and satellites: formation.

## 1 INTRODUCTION

The number of exoplanets has substantially increased in recent years. At the time of writing, over 3500 exoplanets (see [www.exoplanet.eu](http://www.exoplanet.eu)) are discovered, mostly through radial velocity and transiting surveys. In particular, as of Nov. 10, 2015, Kepler mission released approximately 1030 confirmed planets, along with over 4696 transiting planetary candidates (Fressin et al. 2013). This may imply that the planets appear to be very common, orbiting other stars beyond our own solar system.

The observations show that close-in (short-period) terrestrial planets are typically common in the exoplanetary systems. Roughly speaking, one third to half of solar-type (FGK) stars can host at least one planet with a mass less than  $10 M_{\oplus}$  and an orbital period ranging from 50 to 100 days (Howard et al. 2010; Mayor et al. 2011). The frequency of short-period terrestrial planets is at least as high around M stars as around FGK stars, or even higher (Howard et al. 2012; Bonfils et al. 2013; Fressin et al. 2013). These terrestrial planets are usually found in multi-planet systems on compact but non-resonant orbits (Udry et al. 2007; Lovis et al. 2011; Lissauer et al. 2011). However, from the statistical results of Kepler release data, a great many of planet pairs in the systems are observed to be in near-resonant configurations (Zhang et al. 2010; Lee et al. 2013; Martí et al. 2013; Wang & Ji

2014; Zhang et al. 2014), such as the 4:2:1 MMRs. For example, Kepler-238 (Rowe et al. 2014) and Kepler-302 (Rowe et al. 2014) systems harbor close-in giant planets in near mean motion resonance (MMR) configuration with other planets. Therefore, these exciting observations motivate us to explore and understand the formation and evolution of the planetary systems, especially to investigate the short-period terrestrial planet formation and the configuration formation of the 4:2:1 MMRs.

Several models have been proposed to explain the formation of close-in terrestrial planets (Raymond et al. 2008), and the formation scenarios include in situ accretion, orbital migration arising from planetary embryos (type I migration (Goldreich & Tremaine 1980)) and gas giant planets (type II migration (Lin & Papaloizou 1986)), dynamical instabilities in systems of multiple gas giant planets, tidal circularization of eccentric terrestrial planets, and photo-evaporation of close-in giant planets. For the systems that are composed of short-period terrestrial planets, their protoplanetary disks are suggestive of very massive (Raymond et al. 2008; Hansen & Murray 2012, 2013; Chiang & Laughlin 2013; Raymond & Cossou 2014), thus the planets can accrete in situ from a large number of planetesimals and planetary embryos in the disk. The formation and final configuration of close-in terrestrial planets are closely related to the strength of type-I migration, and the suppression of type I migration is required in case of in-situ super-Earths formation (Ogihara & Ida 2009; Ogihara et al. 2015). The observed systems of hot super-Earths mostly can con-

\* E-mail: jijh@pmo.ac.cn

tain 20 - 40  $M_{\oplus}$  in mass within a fraction of an AU of the host star (Batalha et al. 2013). Star-planet tidal interactions may play a role in circularizing planets in highly-eccentric orbits and therefore reduce their semi-major axis in the evolution (Ford & Rasio 2006; Fabrycky & Tremaine 2007; Beaugé & Nesvorný 2012; Dong & Ji 2013). However, Raymond et al. (2008) suggested that tidal effect can produce hot super-Earths, but only for those relatively massive planets ( $\gtrsim 5M_{\oplus}$ ) with very small perihelion distances ( $\lesssim 0.025$  AU), and even then the inward movement in orbital distance is only 0.1-0.15 AU at most, therefore tides are not strong enough to move many of the Kepler planets to the nowadays observed separations, and additional dissipative processes are at play (Lee et al. 2013).

Alternatively, terrestrial planet may form inside a migrating giant planet (Raymond et al. 2006). Gas-giants can shepherd planetesimals and embryos interior to their orbits as they migrate inward, which can further collide and merge into Earth-like planets (Zhou et al. 2005). Mandell et al. (2007) showed materials that have been shepherded interior to the migrating giant planet by moving MMRs can accrete into close-in terrestrial planets. In addition, Izidoro et al. (2014) indicated that fast-migrating super-Earths only weakly perturb the planetesimals disk and planetary embryos, whereas slowly migrating super-Earths shepherd rocky material interior to their orbits in resonances and push toward the star. Moreover, the orbital migration and planet-planet scattering play a vital role in producing short-period terrestrial planets (Brunini & Cionco 2005; Terquem & Papaloizou 2007; Raymond et al. 2008; Cossou et al. 2014). According to core-accretion model, the planetary embryos in the terrestrial planet formation region, and the solid cores of giant planets, are both formed within  $\sim 1$  Myr from kilometer-sized planetesimals (Safronov 1969; Wetherill 1980). Subsequently, the massive solid cores can further accrete gas from the protoplanetary disk to form gas-giants (Kokubo & Ida 2002; Ida & Lin 2004) at Myr timescale, before the disk disperses (Haisch et al. 2001). In the late stage of planet formation, after the gas disk clears, the giant planets ceases migrating, the numerous planetesimals and planetary embryos in the disk become turbulent due to dynamical stirring by gas-giants over hundreds of Myrs or even longer. Consequently, frequent orbital crossings and giant impacts are likely to occur, which may eventually yield short-period Earth-like planets (Chambers 2001; Raymond et al. 2004; Zhang & Ji 2009; Ji et al. 2011).

Raymond et al. (2006) investigated terrestrial planets formation under type II migration and in the model they included a giant planet and gas drag. Based on Raymond et al.'s model, Mandell et al. (2007) further considered an additional non-migrating giant planet. In our earlier study, we have investigated the 3:2 and 2:1 MMRs configuration formation (Wang & Ji 2014) in the system observed by Kepler mission, and simply considered the planets with their nominal masses that are over a few Earth masses without any growth (Wang et al. 2012; Wang & Ji 2014). In the present work, we aim to explore terrestrial planet formation especially in the system with 4:2:1 configuration under migration by performing N-body simulations. In short, we have carried out two kinds of simulations, where in the first model we include the presence of giant planet and as a comparison, in the second model we consider the configuration formation in the system with only terrestrial planets.

The paper is structured as follows. In Section 2, we describe the adopted models of planetary formation, including the disk model and the planetary migration scenarios. In Section 3 we present numerical setup and major results of our investigation. Fi-

nally, we summarize the outcomes and give a brief discussion in Section 4.

## 2 MODELS

Following the empirical minimum-mass solar nebula (MMSN, Hayashi 1981) model, the surface density of solid disk at stellar distance  $a$  is described as

$$\Sigma_d = 10 f_d \gamma_{ice} \left( \frac{a}{1 \text{ AU}} \right)^{-3/2} \text{ g cm}^{-2}, \quad (1)$$

where  $f_d$  and  $\gamma_{ice}$  are the solid and the volatile enhancement factor, respectively.  $\gamma_{ice}$  is 4.2 exterior to the snow line or 1 interior to snow line. The profile of gas density is given as

$$\Sigma_g = 2.4 \times 10^3 f_g f_{dep} \left( \frac{a}{1 \text{ AU}} \right)^{-3/2} \text{ g cm}^{-2}, \quad (2)$$

where  $f_g$  and  $f_{dep}$  are the gas enhancement factor and gas depletion factor, respectively.  $f_{dep} = \exp(-t/\tau_{dep})$ , where  $t$  is the time and the timescale  $\tau_{dep}$  is about few million years (Haisch et al. 2001). Herein we adopt  $\tau_{dep} = 10^6$  yr. The inner edge of the gas disk locates at 0.1 AU.

As they are considered small bodies in our simulations, the planetesimals will be affected by the aerodynamical drag of the gas around them (Adachi et al. 1976; Tanaka & Ida 1999). The force that a planetesimal with a mass  $m$  will suffer from aerodynamical drag is written as

$$\mathbf{F}_{aero} = -\frac{1}{2} C_D \pi S^2 \rho_g |\mathbf{U}| \mathbf{U}, \quad (3)$$

where  $\mathbf{U} = \mathbf{V}_k - \mathbf{V}_g$  is the relative velocity between the planetesimal's Keplerian motion  $\mathbf{V}_k$  and the gas motion  $\mathbf{V}_g$ .  $C_D$  is the drag coefficient. If an object has a large Reynold number,  $C_D$  can be taken as 0.5.  $S$  and  $\rho_g$  are the planetesimal's radius and gas density, respectively.

For a planetary embryo embedding in the gaseous disk, their mutual interactions will lead to an eccentricity damping of the embryo with a timescale  $\tau_{damp}$  written as (Cresswell & Nelson 2006)

$$\tau_{damp1} = \left( \frac{e}{\dot{e}} \right) = \frac{Q_e}{0.78} \left( \frac{M_*}{m} \right) \left( \frac{M_*}{\Sigma_g a^2} \right) \left( \frac{h}{r} \right)^4 \Omega^{-1} \times \left[ 1 + \frac{1}{4} \left( \frac{r}{h} \right)^3 \right], \quad (4)$$

where  $h$ ,  $r$ ,  $\Omega$ , and  $e$  are disk scale height, distance from central star, Keplerian angular velocity, and the eccentricity of the embryo, respectively.  $Q_e = 0.1$  is a normalized factor in association with hydrodynamical simulation results. Moreover, the angular momentum exchange between the embryos and the gas disk will result in orbital migration of planets. When the planets are less massive, they will undergo type I migration, whereas they grow large enough, they will experience type II migration (Ida & Lin 2004).

The timescale of type II migration can be assessed using linear model and the net loss on embryo (Goldreich & Tremaine 1979; Ward 1997; Tanaka et al. 2002) is expressed as

$$\tau_{\text{migI}} = \frac{a}{|\dot{a}|} = \frac{1}{(2.7 + 1.1\beta)} \left( \frac{M_*}{m} \right) \left( \frac{M_*}{\Sigma_g a^2} \right) \times \left( \frac{h}{a} \right)^2 \left[ \frac{1 + \left( \frac{er}{1.3h} \right)^5}{1 - \left( \frac{er}{1.1h} \right)^4} \right] \Omega^{-1}, \quad (5)$$

where  $e$ ,  $r$ ,  $h$ , and  $\Omega$  are the same meaning as given in Equation 4. Using the gas density profile in Equation (2), we can achieve  $\beta = -d \ln \Sigma_g / d \ln a = 1.5$ .

Recent work showed that type I migration can be directed either inward or outward depending on different planetary and gas disk properties (Cossou et al. 2013), but in general, outward type I migration can simply at work when the mass of the planets can be several  $M_\oplus$  (Cossou et al. 2014; Lega et al. 2014), which are much larger than the embryos and planetesimals in our model, so we do not consider outward type I migration in this work.

The planet will experience type II migration when a planet grows to a massive one ( $M \geq M_{\text{crit}}$ ) in the viscous disk (Lin & Papaloizou 1993). The timescale of type II migration is described as (Ida & Lin 2008)

$$\tau_{\text{migII1}} \simeq 5 \times 10^5 f_g^{-1} \times \left( \frac{C_2 \alpha}{10^{-4}} \right)^{-1} \left( \frac{m}{M_J} \right) \left( \frac{a}{1 \text{ AU}} \right)^{1/2} \left( \frac{M_*}{M_\odot} \right)^{-1/2},$$

$$\tau_{\text{migII2}} = \frac{a}{|\dot{a}|} = 0.7 \times 10^5 \left( \frac{\alpha}{10^{-3}} \right)^{-1} \left( \frac{a}{1 \text{ AU}} \right) \left( \frac{M_*}{M_\odot} \right)^{-1/2}, \quad (6)$$

where  $\alpha$  and  $C_2$  are efficiency factor of angular momentum transport and reduce factor. Herein  $C_2 \alpha = 10^{-4}$ .  $\tau_{\text{migII1}}$  is fit to the case that the planet mass is comparable to the entire mass of the gas disk. While the planet mass is lower than the mass of the gas disk,  $\tau_{\text{migII2}}$  is the right fit. We adopt an empirical formula for the eccentricity damping from the gas disk,  $(\tau_{\text{damp2}})^{-1} = (\dot{e}/e) = -K|\dot{a}/a|$  (Lee & Peale 2002). Herein, we choose  $K=10$ . The critical mass of planet that can produce a gap is given as

$$M_{\text{crit}} \simeq 30 \left( \frac{\alpha}{10^{-3}} \right) \left( \frac{a}{1 \text{ AU}} \right)^{1/2} \left( \frac{M_*}{M_\odot} \right) M_\oplus. \quad (7)$$

In this work, besides mutual gravitational interaction among the objects in the system, we also consider the orbital migration, eccentricity damping and aerodynamical drag of planetary embryo (planetesimal). The acceleration of the planet or planetary embryo (planetesimal) with mass  $m_i$  is expressed as

$$\frac{d}{dt} \mathbf{V}_i = -\frac{G(M_* + m_i)}{r_i^2} \left( \frac{\mathbf{r}_i}{r_i} \right) + \sum_{j \neq i}^N G m_j \left[ \frac{(\mathbf{r}_j - \mathbf{r}_i)}{|\mathbf{r}_j - \mathbf{r}_i|^3} - \frac{\mathbf{r}_j}{r_j^3} \right] + \begin{cases} \mathbf{F}_{\text{damp1}} + \mathbf{F}_{\text{aero}} + \mathbf{F}_{\text{migI}} & (\text{for planetesimals/embryos}) \\ \mathbf{F}_{\text{damp2}} + \mathbf{F}_{\text{migII}} & (\text{for giant planets}) \end{cases} \quad (8)$$

where

$$\mathbf{F}_{\text{damp1,2}} = -2 \frac{(\mathbf{V}_i \cdot \mathbf{r}_i) \mathbf{r}_i}{r_i^2 \tau_{\text{damp1,2}}},$$

$$\mathbf{F}_{\text{migI}} = -\frac{\mathbf{V}_i}{2\tau_{\text{migI}}}, \quad (9)$$

$$\mathbf{F}_{\text{migII}} = -\frac{\mathbf{V}_i}{2\tau_{\text{migII}}},$$

where  $\mathbf{r}_i$  and  $\mathbf{V}_i$  represent the position and velocity vectors of planet  $m_i$  and all vectors are given in stellar-centric coordinates.

## 3 NUMERICAL SIMULATIONS AND RESULTS

### 3.1 Initial conditions

In our simulations, all bodies are assumed to be initially in coplanar and near-circular trajectory orbiting the central star, where the argument of pericenter, mean anomaly, and longitude of ascending node are randomly distributed between  $0^\circ$  to  $360^\circ$ , respectively. In total, five runs were carried out for the investigation of planetary formation.

In simulation S1-S5, the planetary system is composed of the host star, one or two giant planets, and 2000 equal-mass planetesimals. As shown in Table 1 and Equation (8), each planetesimal performs aerodynamical drag, eccentricity damping, Type I migration and the gravitational perturbations from Jupiter or Saturn and other planetesimals in the system. The giant planets are modeled to suffer from eccentricity damping, Type II migration, and the interaction from the planets and small bodies. In several runs, the giant planets are assumed to be fixed about the original region without migration. In the following, we will briefly summarize each case.

In these simulations, we mainly explore the terrestrial planetary formation under the circumstance of the existence of giant planets. Thus, in each simulation we start with a swarm of planetesimals, together with one or two giant planets in the system, orbiting the central star. The initial positions for Jupiter and Saturn are set to be 5.0 AU and 9.54 AU, respectively. Originally, the inner region of the system consists of 2000 planetesimals that each owns a mass of  $5 \times 10^{-3} M_\oplus$ , thereby leading to an entire mass of the planetesimal disk of  $10 M_\oplus$ . Herein for all cases, the planetesimals are initially distributed in the region [0.5, 3.78] AU.

S1: In this scenario, the planetary system comprises the host star, the planetesimals, and one Jupiter-mass planet. The model assumes that the giant planet suffers from type II migration over the dynamical evolution.

S2: The initials parameters for Jupiter and planetesimals are the same as those given in S1. As a comparison, in this simulation the model does not account for type II migration for Jupiter.

S3, S4 and S5: in this three runs, the initial system consists of the host star, the planetesimals, two giant planets – Jupiter and Saturn. In simulation S3, both Jupiter and Saturn do not migrate inward but remain stable orbits. In simulation S4 and S5, both Jupiter and Saturn are allowed to migrate inward in the dynamical evolution.

We integrate Equation (8) using a hybrid symmetric algorithm in MERCURY package (Chambers 1999). However, we have modified codes to incorporate gas drag and orbital migration scenarios for our simulation. In these runs, mutual interactions of all bodies are fully taken into account. Two bodies are considered to be in collision stage whenever their distance is less than the sum of two physical radii (Chambers 1999). If two objects collide each other, they can merge and form a single larger body without any fragmentation. In our simulation, each run is integrated for 2 - 100 Myr with a time step of 2 days and a Bulirsch-Stoer tolerance of  $10^{-12}$ . As usual, when the simulation ends up, the variations of energy and angular momenta are  $10^{-3}$  and  $10^{-11}$ , respectively.

**Table 1.** The initial conditions of the runs. The meaning of Force is given by Equation 8.

Name	Mass of planetesimal $M_{\oplus}$	No. Planetesimals	Jupiter Yes or Not	Saturn Yes or Not	Force on giant planets
S1	$5 \times 10^{-3}$	2000	Y	N	$F_{\text{migII}}$
S2	$5 \times 10^{-3}$	2000	Y	N	No migration
S3	$5 \times 10^{-3}$	2000	Y	Y	No migration
S4	$5 \times 10^{-3}$	2000	Y	Y	$F_{\text{migII}}$
S5	$5 \times 10^{-3}$	2000	Y	Y	$F_{\text{migII}}$

**Table 2.** The statistics of the final destination of the planetesimals in each runs.

Name	Time Myr	Percentage of mass (inside 0.1 AU)	Percentage of Mass (beyond 5 AU)	Saturn Yes or Not	Force on giant planets
S1	5	79.5%	8%	N	$F_{\text{migII}}$
S2	3.9	14.1%	0	N	No migration
S3	3.7	17.9%	0	Y	No migration
S4	5	50.5%	14.8%	Y	$F_{\text{migII}}$
S5	5	36.9%	5.9%	Y	$F_{\text{migII}}$

### 3.2 Terrestrial planets formation with giant planets

The simulations of S1-S5 exhibit classical terrestrial planetary accretion scenarios in their late stage formation (Chambers 2001; Raymond et al. 2004, 2006; Fogg & Nelson 2005, 2009).

#### 3.2.1 Terrestrial planets formation with one giant planet

Figure 1 shows the orbital evolution of the planetesimals and the Jupiter-mass planet in the first 5 Myr for simulation S1. At an early time, the Jupiter-mass planet migrates inward in the disk, thereby giving rise to the planetesimals nearby the giant planet to either be scattered outward into high-eccentric orbits (Mandell & Sigurdsson 2003) or shepherded inward by the giant planet's moving mean motion resonances (Tanaka & Ida 1999; Fogg & Nelson 2005). The buildup of inner material induces rapid growth of two close-in planets within a few Myr. At 5 Myr, five terrestrial planets form inside 0.1 AU. The total mass of these five planets is  $7.95 M_{\oplus}$ , corresponding to  $\sim 80\%$  of the initial building materials set in the simulation. There are 16 planetesimals that were scattered to orbits beyond 5 AU, the total mass of them is  $\sim 0.08 M_{\oplus}$ , the final destination of the planetesimals is shown in Table 2. The simulation S1 continues evolving for 100 Myr. By the end of 100 Myr, most of the planetesimal in the initial disk have been nearly cleared up by ejection or collision scenarios, arising from frequent orbital crossings over the chaotic evolution. We observe that there also exist a couple of moderate-eccentric planetesimals which are not involved in accretion process beyond  $\sim 5$  AU for the remaining disk.

Moreover, we find that two terrestrial planets with a mass of  $5.48 M_{\oplus}$  and  $1.62 M_{\oplus}$  are eventual survivors in the system, locating at 0.069 AU and 0.104 AU, respectively. These two terrestrial planets and the Jupiter form a 4:2:1 MMR orbital configuration at  $\sim 10$  Myr, as shown in Figure 2. The discovery of the exoplanets shows that the planetary systems in the universe are quite diverse. Our simulations present very interesting results, which may provide some clues to future observations for such systems.

Our simulation S1 is similar with the work in Raymond et al. (2006) that investigated habitable terrestrial planet formation under a migrating giant planet. In their model, they adopted a higher mass of  $17 M_{\oplus}$  and a more extended planetesimal disk that arranges from 0.25 to 10 AU. They found that hot Earths can form interior to a migrating giant due to the shepherding effect, and in

some cases water-rich earth-mass planet can form outside the migrating giant, located inside the habitable zone. Simulation S1 also shows similar shepherd mechanism, as shown in Figure 1. Interestingly, the two inner terrestrial planets, as well as the migrating giant planet, are discovered to finally form a 4:2:1 MMR orbital configuration. However, we do not observe material around the habitable zone. In simulation S1, the massive giant planet sweeps away or accrete most of the materials along its pathway when it migrates inward. Furthermore, we point out that such material depletion of migrating giant planet can be observed in our simulation S5 (Figure 7), in which the system contains two migrating giants.

Initials in simulation S2 are the same as those in S1, however in this model we simply do not let Jupiter undergo type II migration. Figure 3 shows the orbital evolution of the planetesimals and the Jupiter-mass planet for simulation S2. In similar case, the planetesimals are quickly excited due to their mutual gravitation, along with that of the Jupiter-mass planet locating at 5.0 AU. The objects, involved in the 3:1 MMR at 2.50 AU, 2:1 MMR at 3.28 AU, and the 5:3 MMR at 3.70 AU, are stirred within 0.1 Myr. This trend can be clearly seen by the rise of the eccentricities of the planetesimals at these locations as shown in Figure 3. All stuff in the planetesimal disk exterior to the 3:2 resonance at 3.97 AU is quickly removed from the system via collision and ejection resulting from the giant planet. In the time evolution, the planetesimals' eccentricities can increase and the system becomes chaotic when the eccentricities are larger enough. The bodies in the inner disk begin to grow via accretionary collisions within 1 Myr. The larger bodies tend to have smaller eccentricities and inclinations, due to the dissipative effects of dynamical friction. At 3.9 Myr, there are four less massive terrestrial planets (as compared to S1) with a mass of  $0.15 - 0.51 M_{\oplus}$  formed in the region  $[0.07, 0.095]$  AU. The entire mass of four terrestrial planets is  $1.41 M_{\oplus}$ , corresponding to  $\sim 14.1\%$  of the total initial materials as shown in Table 2.

In comparison, we can see that an inward-migrating giant planet can significantly increase the accretion rate in the inner part of planetesimal disk by the shepherd effect. Meanwhile, it can scatter the bodies in the inner disk to the outer disk.



**Table 3.** Physical parameters of the 3 runs that form 4:2:1 MMR at 100 Myr and comparison with exoplanet systems.

Name	Mass	Radius	Period	$a$	$e$	Name	Mass <sup>a</sup>	Radius	Period	$a$	$e$
	$M_{\oplus}$	$R_{\oplus}$	day	AU			$M_{\oplus}$	$R_{\oplus}$	day	AU	
S1 Planet 1	5.48	2.47	6.62	0.069	0.001	Kepler-238 c	6.0	2.39	6.16	0.069	-
S1 Planet 2	1.62	1.65	12.25	0.104	0.038	Kepler-238 d	10	3.07	13.23	0.115	-
S1 Jupiter	333.55	9.72	24.91	0.167	0.000	Kepler-238 e	77	8.26	23.65	0.169	-
S4 Saturn	95.69	6.41	5.64	0.062	0.001	Kepler-302 b	18	4.06	30.18	0.193	-
S4 Planet 1	5.05	2.41	11.72	0.101	0.012	-	-	-	-	-	-
S4 Jupiter	333.46	9.72	24.91	0.167	0.001	Kepler-302 c	180	12.45	127.28	0.503	-
S5 Planet 1	3.69	2.16	10.02	0.0911	0.142						
S5 Jupiter	333.02	9.71	20.15	0.1449	0.025						
S5 Saturn	95.12	6.40	40.79	0.2315	0.014						

<sup>a</sup> Kepler planetary masses estimated with Eq. (1) in (Lissauer et al. 2011b).

### 3.2.2 Terrestrial planets formation with two giant planets

In the following, we will present the simulation outcomes of the terrestrial planetary formation co-existence with two giant planets in the planetary systems.

In simulation S3, two giant planets, which bear a Jupiter or Saturn mass, respectively, do not perform type II migration in the simulation. Therefore, similar to simulation S2, the planetesimals in the disk can be swiftly excited due to gravitational perturbations from two giant planets. In particular, the bodies, which are involved in the MMR with the Jupiter-mass planet, then acquire moderate eccentricities within 0.1 Myr. As compared to Jupiter, the Saturn-mass planet plays a less dominant role in the mass accretion of planetesimals in forming terrestrial planets. In the meanwhile, owing to the co-existence of two giant planets, the terrestrial formation process can be speeded up although Jupiter and Saturn do not deviate much from their initial orbits in this run. Figure 4 shows temporal orbital evolution of all the planetesimals and the giant planets in simulation S3. At  $\sim 2$  Myr, three terrestrial planets are yielded with a mass in the range  $0.10 - 0.57 M_{\oplus}$ , and they orbit in the broad region from 0.07 AU to 1 AU. At the time of 3.7 Myr, the entire mass of four terrestrial planets formed inside 0.1 AU is  $1.79 M_{\oplus}$ , occupying 17.9% of the initial mass of the planetesimal disk. Similar with the simulation S2, there is no planetesimal beyond 5 AU.

In order to investigate the role of type II migration, we have performed two additional runs for the systems composed of two giant planets, Simulation S4 and S5. In this two runs, both Jupiter and Saturn undergo type II migration. Our results provide evidence that terrestrial formation may take place in the inner region of the planetary systems (Fogg & Nelson (2005); Mandell et al. (2007); Fogg & Nelson (2009)). However, new runs further show some interesting outcomes - the 4:2:1 MMR configurations are formed for these systems.

Figure 5 shows temporal orbital evolution of all the planetesimals and giant planets. According to Equation 6,  $\tau_{\text{migIII}}$  is proportional to the planetary mass, thus we learn that Saturn migrates faster than Jupiter does, indicating that there would be a possibility for two giant planets to rendezvous in the system. At 0.02 Myr, Jupiter's eccentricity is gradually pumped up to 0.30 due to gravitational interaction from Saturn when it moves inward closer to the Jovian planet.

At 0.036 Myr, Jupiter and Saturn reach the orbit at 5.75 AU and 3.58 AU, respectively, indicating that they pass through a 1:2 mean motion resonance. This resonance crossings may have excited the orbital eccentricities of the planets which cross the resonance (e.g., Tsiganis et al. 2005; Morbidelli et al. 2007). Thus,

the orbital crossing between two giant planets happens within several thousand years and brings about fairly chaotic behaviors for them. Hence, a sudden jump in the Jupiter's eccentricity occurs up to  $\sim 0.72$  at 0.037 Myr, whereas Saturn may obtain a moderate eccentricity right after the close encounter but its eccentricity is quickly damped by the gas disk. From the simulations, we find that Jupiter experienced close encounters with Saturn at the maximum star-centric distance at  $\sim 2.41$  AU, which leads to strong interaction between them. From  $\sim 0.037$  Myr to 0.04 Myr, note that the semi-major axis of Jupiter drops down from 3.58 AU to 1.63 AU, whereas that of Saturn dramatically decreases from 5.75 AU to 0.45 AU. Furthermore, such chaotic motions for Jupiter and Saturn trigger catastrophic fate for the planetesimals in the system, where most of their orbits are severely excited and scattered. As Figure 6 shown, the eccentricity of the planetesimal (Planet 1) is first kicked to be 0.88 then falls to 0.13, while its semi-major axis can suddenly increase amount up to 5.18 AU, then soon drop down to 0.26 AU over the time span.

As the two giant planets continue migrating inward, the 2:1 MMR between them is broken up. Subsequently, Saturn is kicked into the region  $\sim 0.1$  AU due to dynamical instabilities. By 10 Myr, the giant planets have moved very close to their central star. In the late stage, the eccentricity of Jupiter is gradually damped by dynamical dissipation. However, an inner terrestrial planet (Planet 1) is excited onto a highly eccentric orbit exterior to the regime of two giant planets, and soon crosses Jupiter's orbit, then finally captured inside the orbits of Jupiter and Saturn. The mass growth for Planet 1 starts from one planetesimal at  $\sim 0.06$  Myr to a super Earth with a mass of  $5.05 M_{\oplus}$  at  $\sim 0.40$  Myr. Finally, Planet 1 remains at 0.101 AU, whereas Saturn and Jupiter cease migrating at 0.062 AU and 0.167 AU, respectively. This planetary system shows a very interesting configuration that a super Earth locates between two giant planets' orbits, and three planets are trapped into a near 4:2:1 MMR (see Figure 8). Accordingly, the residual materials of disk are either removed out of the system or scattered into distant orbits. Their eccentricities rise along with their semi-major axes.

The scenario of S4 shows a resemblance to NICE Model (e.g., Tsiganis et al. 2005; Morbidelli et al. 2007), which proposes that the Late Heavy Bombardment (LHB) – a spike in the impact rate on multiple solar system bodies that lasted from roughly 400 until 700 Myr after the start of planet formation (Tera et al. 1974; Cohen et al. 2000; Chapman et al. 2007) – was triggered by an instability in the giant planets' orbits. In the Nice Model, the orbits of the giant planets would have been in a more compact configuration, with Jupiter and Saturn interior to the 2:1 resonance. In our model of simulation S4, the Jupiter-mass and Saturn-mass planets

can switch each place, similar to the case of Uranus and Neptune in the NICE Model. Raymond et al. (2008b) showed that planet-planet scattering could create MMRs, most of these resonances are indefinitely stable. The previous investigations reported that in a convergent migration scenario for two giant planets in the solar system, the 2:1 MMR could be formed and then disintegrated in the evolution (Morbidelli & Crida 2007b; Zhang & Zhou 2010). Zhang & Zhou (2010b) stated that when Jupiter lies outside Saturn, convergent migration could occur, Saturn is then forced to migrate inward by Jupiter where the two planets are trapped into MMR, and Saturn may move on its tracks of approaching the central star. Furthermore, to apply our model to explain the planetary formation of the systems, we extensively examine the published data by Kepler mission and find a relevant planetary system (Kepler-302) similar to this simulation. Kepler-302 is a system consisting of two planets orbiting a star with a mass of  $0.97 M_{\odot}$ , as shown in Table 3. The outer planet of Kepler-302c is more massive than the inner companion Kepler-302b, and the two planets have approximate sizes as compared with those of the giant planets in simulation S4, whereas their orbital distances from the host star are a bit farther than those of the planets in the present run. Interestingly, the two giant planets of Kepler-302 are nearly close to a 4:1 MMR (Rowe et al. 2014), suggesting that the system may have gone through similar migration process as in our simulation. Therefore, our model herein presents a likely formation scenario for two planets that are close to a 4:1 commensurability, and also provides evidence that terrestrial planet formation under the influence of two giant planets in the compact system.

In simulation S5, although Saturn migrates faster than Jupiter, there is no rendezvous between Saturn and Jupiter. Instead, when Saturn enters the 2:1 MMR orbit of Jupiter at 0.02 Myr, these two giant planets were locked in the 2:1 MMR configuration and they migrate inward together. Figure 7 shows temporal orbital evolution of the simulation S5 for the first 5 Myr. Jupiter's eccentricity is gradually pumped up to 0.30 due to gravitational interaction from Finally, a terrestrial planet of  $3.69 M_{\oplus}$  form inside 0.1 AU. This new terrestrial planet and the two giant planets form a 4:2:1 MMR orbital configuration at  $\sim 5$  Myr. Although Jupiter keeps migrating until 10 Myr in S1, Jupiter ceases its migration at 1.5 Myr and 3.5 Myr in S4 and S5, respectively. This is probably due to the torque from Planet 1, and the torque depends on the edge.

Unlike in simulation S3, in simulation S4 and S5 we can see planetesimals beyond 5 AU due to scattering of inward-migrating giant planets. At 5 Myr, there are about  $1.48 M_{\oplus}$  materials beyond 5 AU in simulation S4, corresponding to 14.8% of the initial total mass. While in simulation S5, there are  $\sim 0.59 M_{\oplus}$  beyond 5 AU.

Figure 8 shows the final configuration in the inner disk for the three runs that have turned on type II migration. Interestingly, all these runs yield 4:2:1 MMR. In simulation S1, two terrestrial planets formed interior to the Jupiter mass planet. The migrating giant increased the accretion rate in the inner disk and cleared all material in its pathway. As a result, there is nothing left between 0.2 to 4.5 AU. In simulation S4, there was an orbital crossing between the migrating Jupiter mass and Saturn mass planets, and such a chaotic event changed the orbital configuration of the two giant planets. Hence, we note that a close-in terrestrial planet formed between two giant planets. There are some residual materials between 0.2 to 5 AU in this run, and this could be a consequence of the quickly orbital change of the two giants at 0.1 Myr, as shown in Figure 6. While in simulation S5, there is no chaotic orbital change of the Jupiter mass and Saturn mass planets. Similar to simulation S1, we see that only one terrestrial planet formed interior to two migrating

giants, and in this case the material of the region between 0.2 and 4.5 AU of the disk was fully cleared by two giant planets.

#### 4 THE EMERGENCE OF 4:2:1 MMRS ONLY WITH TERRESTRIAL PLANETS

The investigations imply that the planetary configurations in association with a near 4:2:1 MMRs would be common in the universe. Herein, we consider two planets with a period ratio in the range of [1.83, 2.18] as a pair near 2:1 MMR (Lissauer et al. 2011b). For example, Jupiter's Galilean moons are known to be locked into a so-called three-body Laplacian resonance (i.e., 4:2:1 MMR) in our solar system. On the other hand, other evidences are found in the exoplanetary systems, in which three planets of the GJ 876 system (Marcy et al. 2001; Rivera et al. 2010; Batygin et al. 2015; Nelson et al. 2016) and Kepler-79 (KOI-152) (Steffen et al. 2010; Wang et al. 2012) are reported to be close to 4:2:1 MMR. In this work, we have provided substantial evidences on this from the simulations. For example, in simulation S1, S4 and S5 of Section 3, we show that the systems initially composed of one or two giant planets can finally produce 4:2:1 MMRs, in which the formed terrestrial planets are involved in. Naturally, a question arises - what if the systems only contain terrestrial planets?

As mentioned previously, the released Kepler outcomes report that a great number of planetary systems harboring terrestrial planets involved in a near 2:1 resonance. Furthermore, a portion of the terrestrial planets discovered by Kepler are in near 4:2:1 resonance. Herein, we further investigate the configuration formation of those systems only with terrestrial planets to understand whether the 4:2:1 MMRs can be produced in such systems. With these purpose, we perform additional runs to explore the systems that simply consist of terrestrial planets through simulations.

In our additional simulations, there are three terrestrial planets initially with masses less than  $30 M_{\oplus}$  around central star, and they are assumed to migrate from the outer region of the system under the effect of the gas disk. The gas density profile is proportional to  $r^{-1}$ , and an empty hole located in the inner region of the system. During the formation process, the terrestrial planets suffer from type I migration and gas damping. The timescales of type I migration and gas damping are shown in Equation (4) and (5), respectively. In total, we carry out seven groups of simulations, and each group contains five runs by considering different speed of type I migration. We add an enhance factor  $\eta$  to the timescale of type I migration. The five runs correspond to  $\eta$  times of typical timescales of type I migration as shown in Equation 5. The values of  $\eta$  are 100, 33.3, 10, 3.3, and 1, respectively. Figure 9 shows one of the runs with typical outcomes. Considering various speed of type I migration, three planets are located at 140, 500, and 1450 d when  $\eta$  is larger than 33.3, otherwise they are located at 100, 250, and 600 d, respectively. The masses of the planets in five groups are 5, 10, and  $15 M_{\oplus}$ , respectively, while in other two groups they are set to be 5, 5, and  $5 M_{\oplus}$ , respectively. In Figure 9, the formation of the innermost, the middle and the outermost planets are marked by the black, red and blue lines, respectively. Panel (a), (b) and (c) show the evolution of the orbital periods, eccentricities, and the period ratios, respectively. Panel (d) and (e) display the 2:1 mean motion resonance angles. In the case with terrestrial planets in the system, they all undergo type I migration. Due to the short timescales for the first two planets, they are trapped into 2:1 MMR first. From Panel (c) in Figure 9, we find that the first and second planets are involved into 2:1 MMR at  $\sim 0.5$  Myr, and then three terrestrial planets are

trapped into 4:2:1 MMRs at  $\sim 1.3$  Myr. From Panel (b), we can learn that when the planet pairs enter into MMRs, their eccentricities are excited, but due to the damping of gas disk, they cannot be stirred up to high values. The 4:2:1 MMR is usually produced when the first planet is trapped in the edge of the holes in the gas disk. The formation process is similar to that mentioned in Pierens & Nelson (2008), the MMR formed when the planet is captured in the gap of the other planet. In addition, we investigate the resonance angles of each pair which are shown in Panel (d) and (e) of Figure 9 and find that  $\theta_{21} = 2\lambda_1 - \lambda_2 - \varpi_1$  librates at  $\sim 0^\circ$ ,  $\theta_{32} = 2\lambda_2 - \lambda_3 - \varpi_2$  librates at  $\sim 0^\circ$ , and  $\theta_{33} = 2\lambda_2 - \lambda_3 - \varpi_3$  librates at  $\sim 180^\circ$ , where the subscript 1 and 2 represent the orbital elements of Planet 1 and 2, respectively. At the end of the simulation, three planets locate at about 11.52, 23.26, 47.17 days, respectively. This configuration is similar to the system Kepler-92 which contains three planets in the orbital periods of 13.75, 26.72, and 49.36 days, respectively. In final, by examining all runs from seven groups, we find that 6 out of 35 runs (17.1%) show three planets are finally involved in 4:2:1 MMRs, whereas 10 runs report that only the two inner planets enter into 2:1 MMR, and two runs for two inner planets in 3:2 MMR. About half of the simulations (48.6%) are not in MMR. Based on our simulations, the proportion that planets pairs trapped near 4:2:1 MMRs appears to be high. There are several reasons that could lead to such results. Firstly, we set the initial orbital separation of planets at  $\sim 20$  Hill radius, which is a little larger than the empirical value of 12 Hill radius (Ida & Lin 2004). In such cases, most of the planets are first trapped by the 2:1 MMRs during their evolution. However, as a comparison, if they are initially in a compact configuration, the probability of the forming planets in 2:1 MMRs will significantly decrease. As shown in the work of Wang & Ji (2014), they found that if the planets pairs were initially in compact configuration at the separations of  $\sim 15$  Hill radius, the probability of 2:1 MMRs decreased to 10% in 50 runs and there was no simulation that three planets were evolved into 4:2:1 MMRs. Secondly, in our simulations we slow down the speed of type I migration for low-mass planets, and this could further explain why two planets are fairly easier to be trapped into 2:1 MMRs. Finally, the final orbital periods of the planets in all simulations are less than 50 days which may be affected by the tidal force that arises from the central star. The tidal effect may lead to the deviation from 2:1 MMRs (Lee et al. 2013). In summary, the above-mentioned factors may play a major role in causing the planets pairs evolved in near 4:2:1 MMRs at a relatively moderate possibility. The simulations in Raymond et al. (2006) utilized the typical speed of type I migration which was very fast, and the embryos were initially located close to each other in compact configuration. These may be the leading differences producing diverse results between our simulations and those of Raymond et al. (2006).

By comparing S1, S4 and S5 simulation containing giant planets and the runs that simply consist of terrestrial planets in this section, we find that the timescales of the planet pairs trapped into MMRs are various for different cases. For the systems that only contain terrestrial planets, the two inner planets are found to be trapped into 2:1 MMRs within 1 Myrs, and the two outer pairs are in resonance at approximately 2-3 Myrs. Therefore, we may conclude that three terrestrial planets are in 4:2:1 MMRs within 3 Myrs on average. In comparison, for the systems consisting of one or two giant planets, the 4:2:1 MMRs emerges at over 2 Myrs when the terrestrial planets complete its mass accretion. Additionally, the eccentricities of planets which is in MMR with giant planets are always excited to be high values, while the eccentricities of planets in systems without giant planets will be suppressed to low values.

## 5 CONCLUSIONS AND DISCUSSIONS

In this work, we have investigated terrestrial planetary formation, especially the configuration formation of a near 4:2:1 MMRs by carrying out two sets of simulations with and without giant planets. From the results we find that 4:2:1 MMRs configuration can be formed in the systems both with and without giant planets. Herein we summarize the major results as follows.

(i) In the first sets, we place one or two giant planets into the initial systems as well as the planetesimals, to understand terrestrial formation in such cases in S1-S5.

In simulations S2 and S3, the giant planets do not undergo migrating in the disk, and the terrestrial formation procedure can be expedited because of the existence of Jupiter-mass and Saturn-mass planets. In final, several low-mass close-in terrestrial planets can be formed as a result of radial mixing and type I migration. In the two runs, there is no 4:2:1 MMRs in the evolution.

In simulation S1, S4, and S5, we place one or two giant planets in the system, which undergo type II migration during the evolution. Thus the planetesimals are shepherded inward, cleared or ejected along with migration of giant planets. The close-in terrestrial planets are yielded with a mass up to several Earth-masses. For simulation S1, we find that two short-period terrestrial planets and one giant planet are finally involved in 4:2:1 MMR, whereas in the runs of S4, and S5, we show that one terrestrial planet and two giant planets enter into the 4:2:1 MMR. The resultant results of S1 and S4 are similar to Kepler-238 and 302 systems in orbital spacing. We examine the mass concentration statistic  $S_c$  and the orbital spacing statistic  $S_s$  (Chambers 2001; Hansen & Murray 2012) for these systems. Comparing the system S1 and Kepler 238, we can note that the orbital spacing statistics are close to each other. Their values for two systems are 1.8 and 2.76, respectively, indicating that S1 and Kepler 238 are similar in the orbital distribution. However, the mass concentration statistics of them differ from each other, and their values are 125.7 and 30.3, respectively. One reason for this difference in mass concentration statistic is that the masses of planets in our simulations are quite uncertain. Herein we adopted an estimated masses from Eq. (1) in Lissauer et al. (2011b). If we can obtain the true masses of planets in S1, the difference of  $S_c$  could be narrowed down. Moreover, we further compare  $S_s$  and  $S_c$  of the system S4 with those of Kepler 302, where  $S_s$  for each system is 5.43 and 4.0, respectively, and  $S_c$  for two systems is 10.4 and 23.3, respectively. This may imply that the system S4 and Kepler 302 have similar orbital distribution. Therefore, we can conclude that S1 and Kepler 238, S4 and Kepler 302 have similar orbital configurations.

The present observations show that there is a lack of companion planets in the observed hot Jupiter systems. However, from our simulation results, we can learn that terrestrial planets can survive inside the inner region of hot Jupiter systems based on our formation scenario. As shown in the system S1, the final formed configuration is similar to that in Raymond et al. (2006). Moreover, if the gas disk is small enough, the hot Jupiter could have terrestrial companions formed in the system (Ogihara et al. 2013). Nevertheless, currently such terrestrial companions in the hot Jupiter systems have not discovered yet, this is because they may be under the detection limit. In the forthcoming, we hope that the hot Jupiter systems with low-mass companions could be discovered with the assistance of the improvement of observational precision and techniques.

(ii) Furthermore, in the second sets, we also explore the 4:2:1 MMRs formation in the case of three terrestrial planets. Under type I migration,  $\sim 17.1\%$  of all runs, indicate that terrestrial planets

are evolved into 4:2:1 MMRs. However, as aforementioned, the probability that planets are trapped into MMRs depends on their initial separation and the speed of type I migration. Comparing the processes with and without giant planets, the timescales that three planet are in 4:2:1 MMRs in systems without giant planets are shorter than systems with giant planets. Additionally, eccentricities are excited to higher values in systems with giant planets than without giant planets.

However, in the treatment of accretion scenario in MERCURY package (Chambers 1999), the collisions between two bodies are assumed to be perfect gravitational aggregations. Leinhardt & Stewart (2012) pointed out that real collisions could suffer from partially accreting collision, hit-and-run impacts, or graze-and-merge events, rather than a complete merger. Recently, Chambers (2013) showed that fragmentation does have a notable effect on accretion under consideration of fragmentation and hit-and-run collisions (Leinhardt & Stewart 2012; Genda et al. 2012). The final stages of accretion are lengthened by the sweep up of collision fragments. The planets that formed with fragmentation in the simulations have smaller masses and lower eccentricities when compared to those simulations without fragmentation. In this sense, the scenarios that include imperfect merger collision will not alter the conclusions of this study. In forthcoming work, we will take into account hit-and-run and fragmentation process in our model for further investigation.

## ACKNOWLEDGMENTS

We thank the anonymous referee for insightful comments and good suggestions that helped to improve the contents. This work is financially supported by National Natural Science Foundation of China (Grants No. 11273068, 11473073, 11503092, 11573073), the Strategic Priority Research Program-The Emergence of Cosmological Structures of the Chinese Academy of Sciences (Grant No. XDB09000000), the innovative and interdisciplinary program by CAS (Grant No. KJZD-EW-Z001), the Strategic Priority Research Program on Space Science, CAS (Grant No. XDA04060901), the Natural Science Foundation of Jiangsu Province (Grant No. BK20141509), and the Foundation of Minor Planets of Purple Mountain Observatory.

## REFERENCES

- Adachi, I., Hayashi, C., & Nakazawa, K., 1976, *Prog. Theo. Phys.* 56, 1756
- Batalha, N. M., et al., 2013, *ApJS*, 204, 24
- Batygin, K., Deck, K., & Holman, M. J., 2015, *AJ*, 149, 167
- Beaugé, C., & Nesvorný, D., 2012, *ApJ*, 751, 119
- Bonfils, X., et al., 2013, *A&A*, 549, A109
- Brunini, A., & Cionco, R. G., 2005, *Icarus*, 177, 264
- Cresswell, P., & Nelson, R. P., 2006, *A&A*, 450, 833
- Chambers, J. E., 1999, *MNRAS*, 304, 793
- Chambers, J. E., 2001, *Icarus* 152, 205
- Chambers, J. E., 2013, *Icarus*, 224, 43
- Chapman, C. R., et al., 2007, *Icarus*, 189, 233
- Chiang, E., & Laughlin, G., 2013, *MNRAS*, 431, 3444
- Cohen, B. A., et al., 2000, *Science*, 290, 1754
- Cossou, C., et al., 2013, *A&A*, 553, L2
- Cossou, C., et al., 2014, *A&A*, 569, A56
- Dong, Y., & Ji, J. H., 2013, *MNRAS*, 430, 951
- Fabrycky, D. & Tremaine, S., 2007, *ApJ*, 669, 1298
- Fogg, M. J., & Nelson, R. P. 2005, *A&A*, 441, 791
- Fogg, M. J., & Nelson, R. P. 2009, *A&A*, 498, 575
- Ford, E. B., & Rasio, F. A., 2006, *ApJL*, 638, L45
- Fressin, F., et al., 2013, *ApJ*, 766, 81
- Genda, H., Kokubo, E., & Ida, S., 2012, *ApJ*, 744, 137
- Goldreich, P., & Tremaine, S., 1979, *ApJ*, 233, 857
- Goldreich, P., & Tremaine, S., 1980, *ApJ*, 241, 425
- Haisch, K. E., Jr., Lada, E. A., & Lada, C. J., 2001, *ApJL*, 553, L153
- Hansen, B. M. S., & Murray, N., 2012, *ApJ*, 751, 158
- Hansen, B. M. S., & Murray, N., 2013, *ApJ*, 775, 53
- Hayashi, C., 1981, *Prog. Theor. Phys. Suppl.*, 70, 35
- Howard, A. W., et al., 2010, *Science*, 330, 653
- Howard, A. W., et al., 2012, *ApJS*, 201, 15
- Ida, S., & Lin, D. N. C., 2004, *ApJ*, 604, 388
- Ida, S., & Lin, D. N. C., 2008, *ApJ*, 673, 487
- Ida, S., & Makino, J., 1992, *Icarus*, 96, 107
- Izidoro, A., Morbidelli, A., & Ramond, S. N., 2014, *ApJ*, 794, 11
- Ji, J. H., Jin, S., & Tinney, C. G., 2011, *ApJL*, 727, L5
- Jin, S., & Ji, J. H., 2011, *MNRAS*, 418, 1335
- Kokubo, E., & Ida, S., 1998, *Icarus*, 131, 171
- Kokubo, E., & Ida, S., 2002, *ApJ*, 581, 666
- Lee M. H., Peale S. J., 2002, *ApJ*, 567, 596
- Lee, M. H., Fabrycky, D., & Lin, D. N. C., 2013, *ApJL*, 774, L52
- Lega, E., et al., 2014, *MNRAS*, 440, 683
- Leinhardt, Z.M., & Stewart, S.T., 2012, *ApJ*, 745, 79
- Lin, D. N. C., & Papaloizou, J. C. B., 1986, *ApJ*, 309, 846
- Lin, D. N. C., & Papaloizou, J. C. B., 1993, in: E.H. Levy & J.I. Lunine (eds.), *Protostars and Planets III*, (Tucson: Univ. Arizona)
- Lissauer, J. J., et al., 2011, *Nature*, 470, 53
- Lissauer, J. J., et al., 2011, *ApJS*, 197, 8
- Lovis, C., et al., 2011, *A&A*, 528, A112
- Mandell, A. M., & Sigurdsson, S., 2003, *ApJ*, 591, L111
- Mandell, A. M., Ramond, S. N., & Sigurdsson, S., 2007, *ApJ*, 660, 823
- Marcy, G. W., et al., 2001, *ApJ*, 556, 296
- Marcy, G. W., et al., 2014, *ApJS*, 210, 20
- Martí, J. G., Giuppone, C. A., & Beaugé, C., 2013, *MNRAS*, 433, 928
- Mayor, M., et al., 2011, *arXiv:1109.2497*
- Morbidelli, A., et al., 2007, *AJ*, 134, 1790
- Morbidelli, A., & Crida, A., 2007, *Icarus*, 191, 158
- Nelson, B. E., et al., 2016, *MNRAS*, 455, 2484
- Ogihara, M., & Ida, S. 2009, *ApJ*, 699, 824
- Ogihara, M., Inutsuka, S. & Kobayashi, H. 2013, *ApJL*, 778, 9
- Ogihara, M., Morbidelli, A., & Guillot, T. 2015, *A&A*, 578, A36
- Pierens, A., & Nelson, R. P., 2008, *A&A*, 482, 333
- Raymond S. N., Quinn T., Lunine J. I., 2004, *Icarus*, 168, 1
- Raymond, S. N., et al., 2006, *Science*, 313, 1413
- Raymond, S. N., et al., 2006, *Icarus*, 183, 265
- Raymond, S. N., et al., 2008, *MNRAS*, 384, 663
- Raymond, S. N., et al., 2008, *ApJ*, 687, L107
- Raymond, S. N., & Cossou, C., 2014, *MNRAS*, 440, L11
- Rivera, E. J., et al., 2010, *ApJ*, 719, 890
- Rowe, J. F., et al., 2014, *ApJ*, 784, 45
- Safronov, V.S., 1969, *Evolution of the Protoplanetary Cloud and Formation of the Earth and the Planets* (Moscow: Nauka)
- Schneider J. et al., 2011, *A&A*, 532, A79
- Steffen, J. H., Batalha, N. M., Borucki, W. J., et al., 2010, *ApJ*, 725, 1226
- Tanaka, H., & Ida, S., 1999, *Icarus*, 139, 350

- Tanaka, H., Takeuchi, T., & Ward, W. R., 2002, *ApJ*, 565, 1257
- Tera, F., et al., 1974, *Earth and Planetary Science Letters*, 22, 1
- Terquem, C., & Papaloizou, J. C. B., 2007, *ApJ*, 654, 1110
- Tsiganis, K., et al., 2005, *Nature*, 435, 459
- Udry, S., et al., 2007, *A&A*, 469, L43
- Wang, J., Xie, J. W., Barclay, T., & Fischer, D. A., 2014, *ApJ*, 783, 4
- Wang, S., Ji, J. H., & Zhou, J. L., 2012, *ApJ*, 753, 170
- Wang, S., & Ji, J. H., 2014, *ApJ*, 795, 85
- Ward, W. R., 1997, *Icarus*, 126, 261
- Wetherill, G. W., 1980, *ARAA*, 18, 77
- Wetherill, G. W., & Stewart, G. R., 1989, *Icarus*, 77, 330
- Zhang, H., & Zhou, J. L., 2010, *ApJ*, 714, 532
- Zhang, H., & Zhou, J. L., 2010, *ApJ*, 719, 671
- Zhang, N., & Ji, J. H., 2009, *Science in China Series G*, 52(5), 794
- Zhang, N., Ji, J. H., & Sun, Z., 2010, *MNRAS*, 405, 2016
- Zhang, X.-J., Li, H., Li, S.-T., & Lin, D. N. C., 2014, *ApJL*, 789, L23
- Zhou, J. L., Aarseth, S. J., et al., 2005, *ApJ*, 631, L85

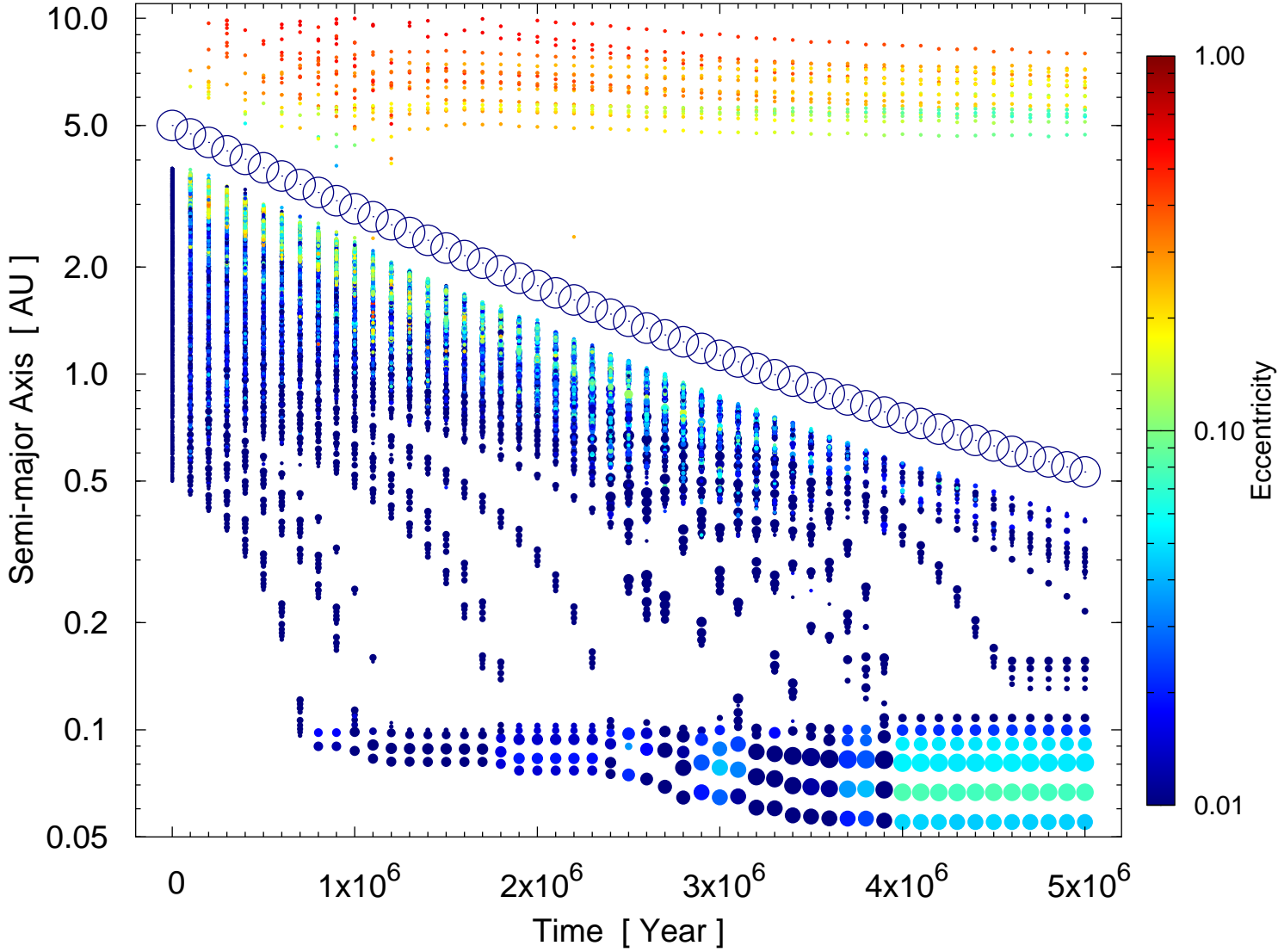


**Figure 1.** Orbital evolution of the planetesimals and Jupiter mass planet in simulation S1. The solid points show the planetesimals. The radii of the planetesimals are proportional to their mass. The color of each point shows the orbital eccentricity. The open circle shows the giant planet. As the Jupiter mass planet migrating inward, the planetesimals at the MMR orbits were excited to high eccentric orbits. Due to the inward-migrating giant planet, planetesimals were shepherded inward and hence the accretion rate in the inner part of the planetesimal disk increases. There are also some planetesimals were scattered to the outer part of the disk. Several terrestrial planets form at 5 Myr.

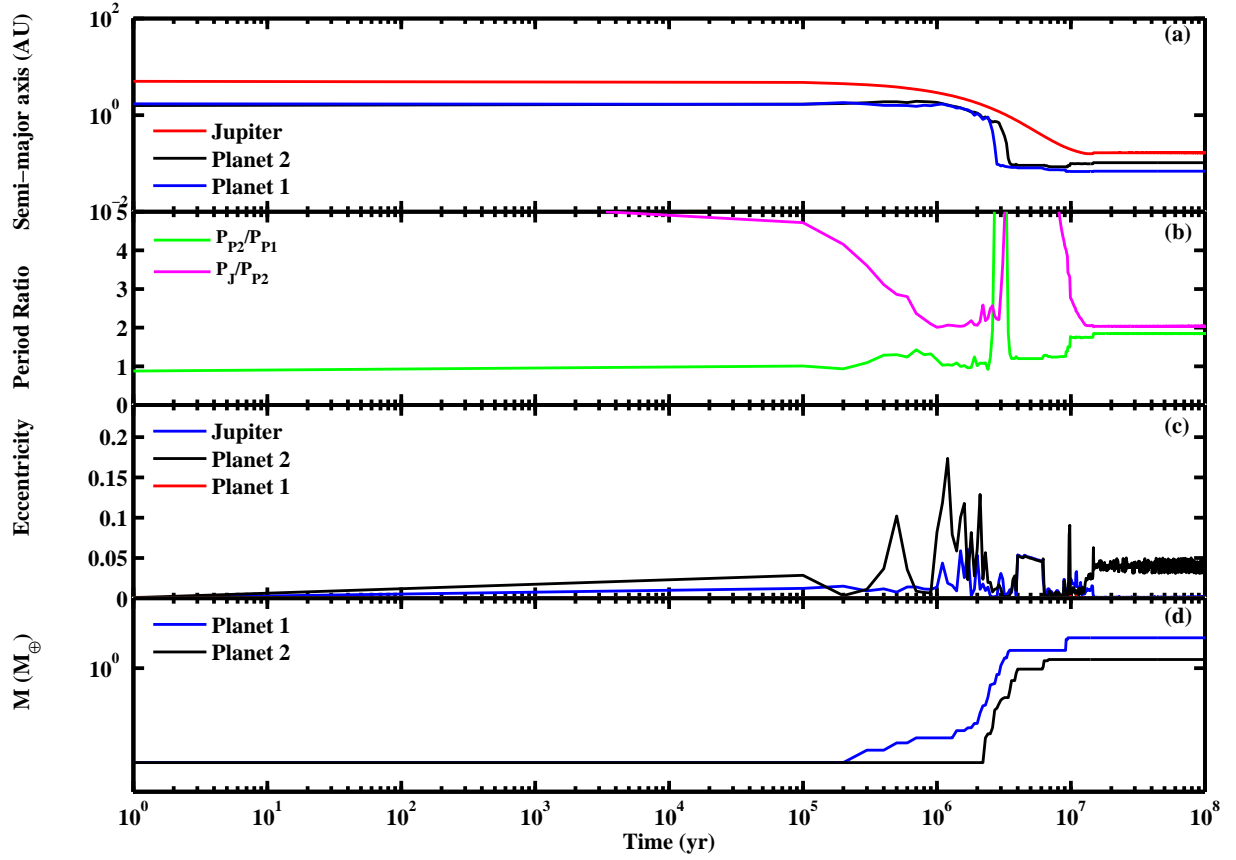


**Figure 2.** Results of the evolution of semi-major axis (upper panel) and eccentricities (lower panel) for simulation S1. Two inner planets undergo type I migration while the outer one under the influence of type II migration. Note that three planets are close to a 4:2:1 MMR.

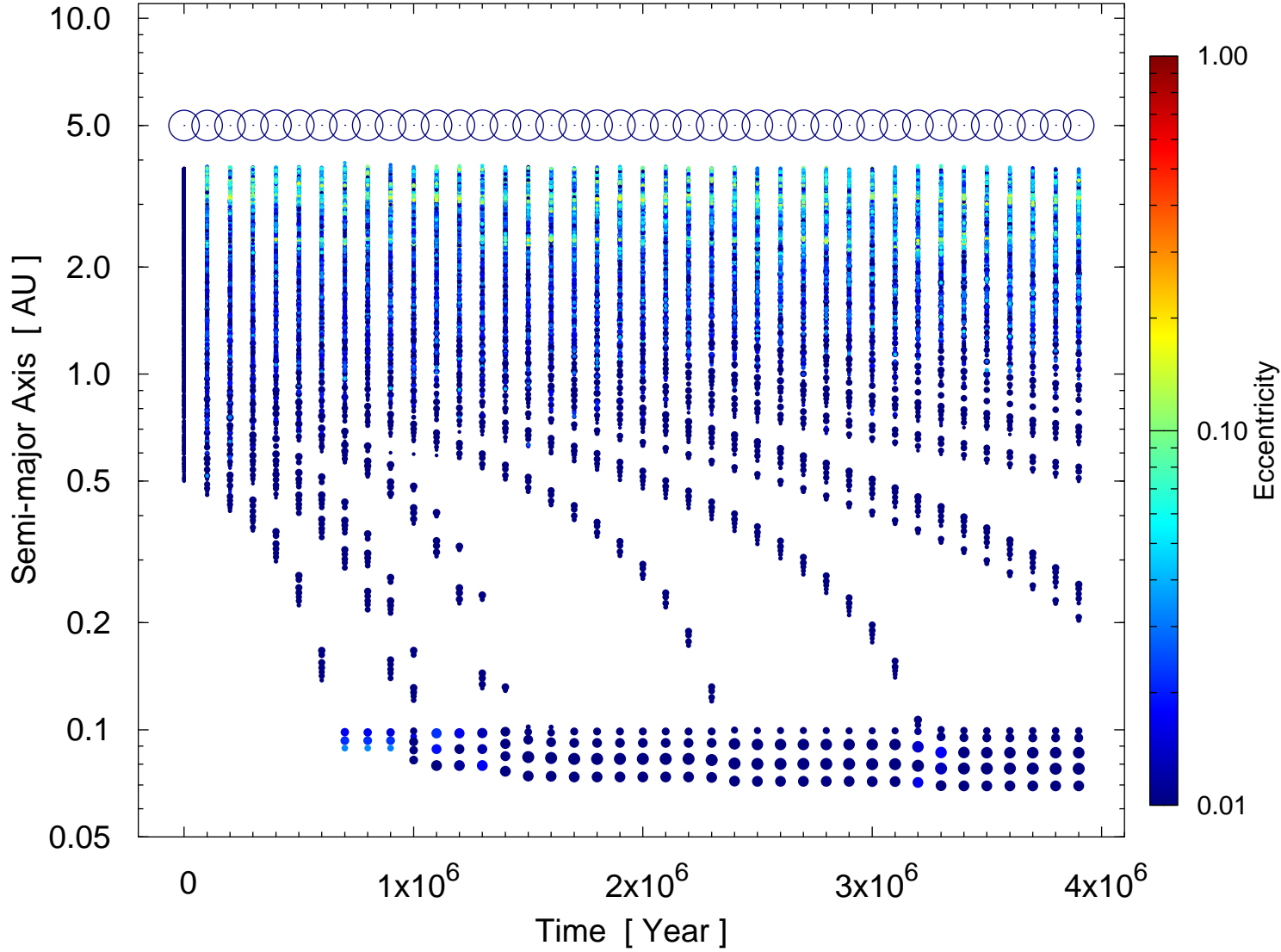


**Figure 3.** Orbital evolution of the planetesimals and Jupiter mass planet in simulation S2. The Jupiter mass planet in this simulation was fixed at 5 AU. The radii of the planetesimals are proportional to their mass. The color of each point shows the orbital eccentricity. We can see the planetesimals at its MMR orbits were excited to high eccentric orbits. The accretion rate in this simulation is much lower than in simulation S1.



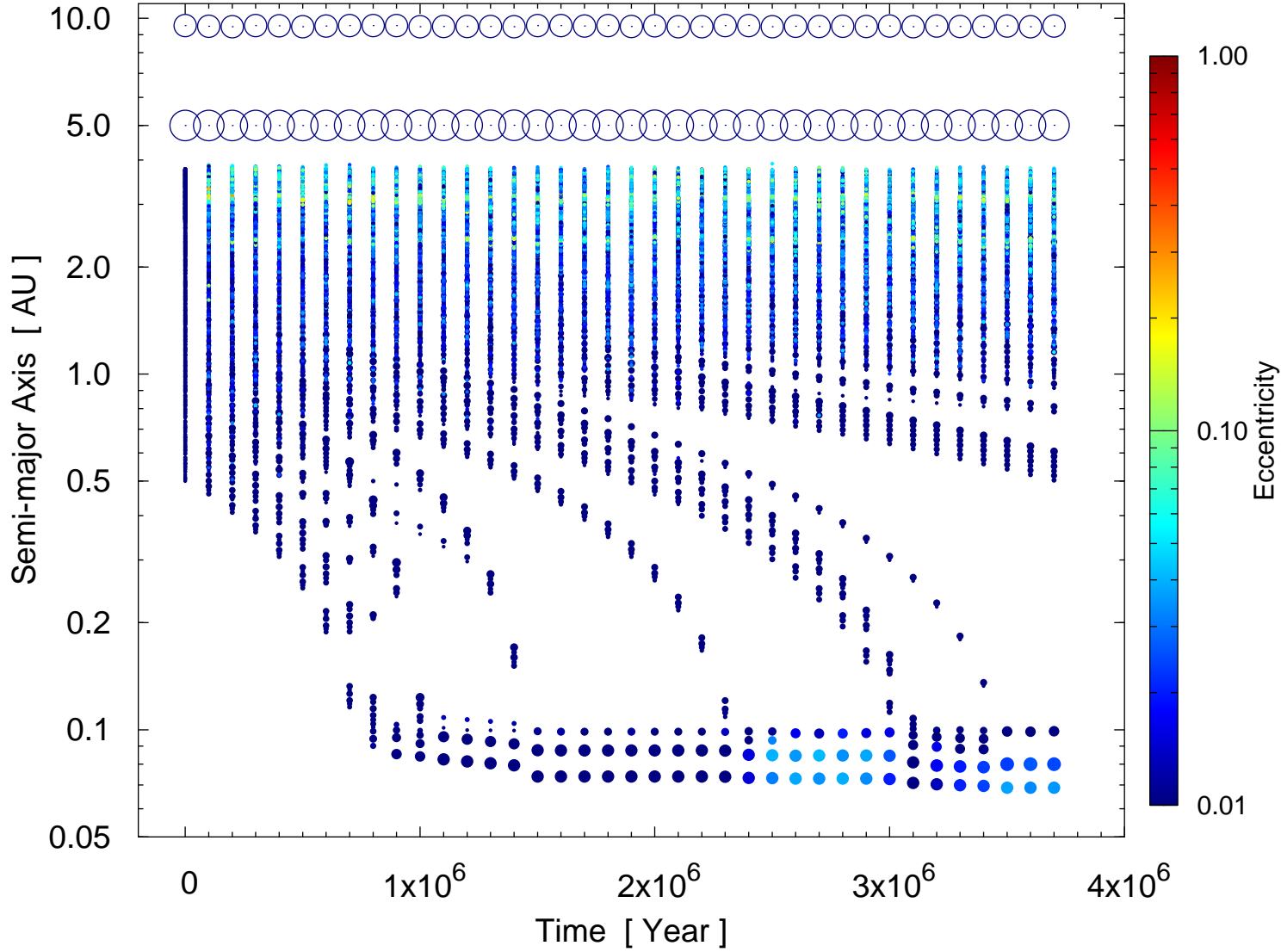


**Figure 4.** Orbital evolution of the planetesimals and two giant planets in simulation S3. The Jupiter and Saturn in this simulation was fixed at 5 and 9.2 AU. The radii of the planetesimals are proportional to their mass. The color of each point shows the orbital eccentricity. The planetesimals at the MMR orbits of the Jupiter mass planet were excited to high eccentric orbits.

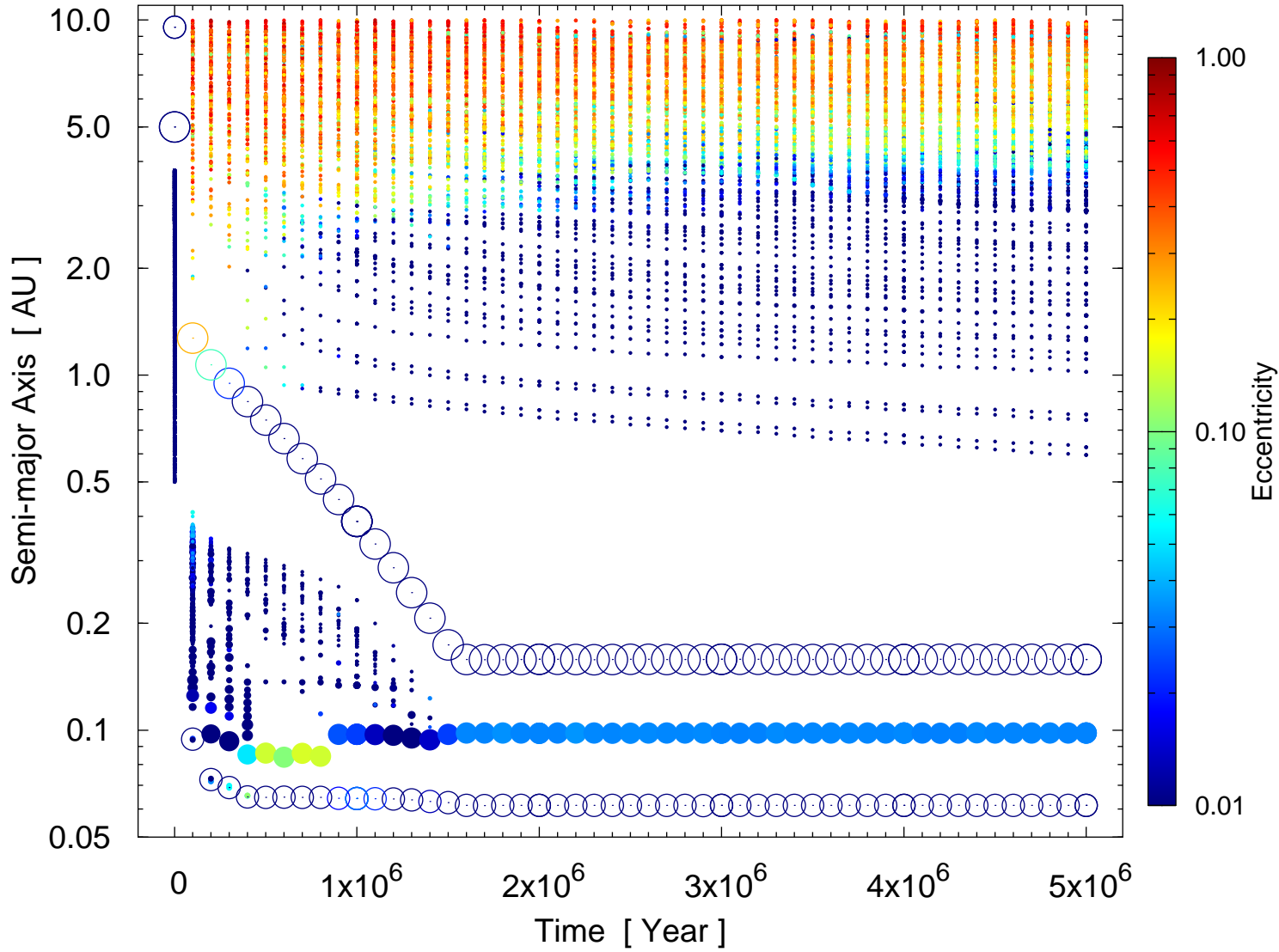


**Figure 5.** Orbital evolution of the planetesimals and two giant planets in simulation S4. The Jupiter and Saturn in this simulation underwent type II migration. The radii of the planetesimals are proportional to their mass. The color of each point shows the orbital eccentricity. Note that three planets are close to a 4:2:1 MMR.

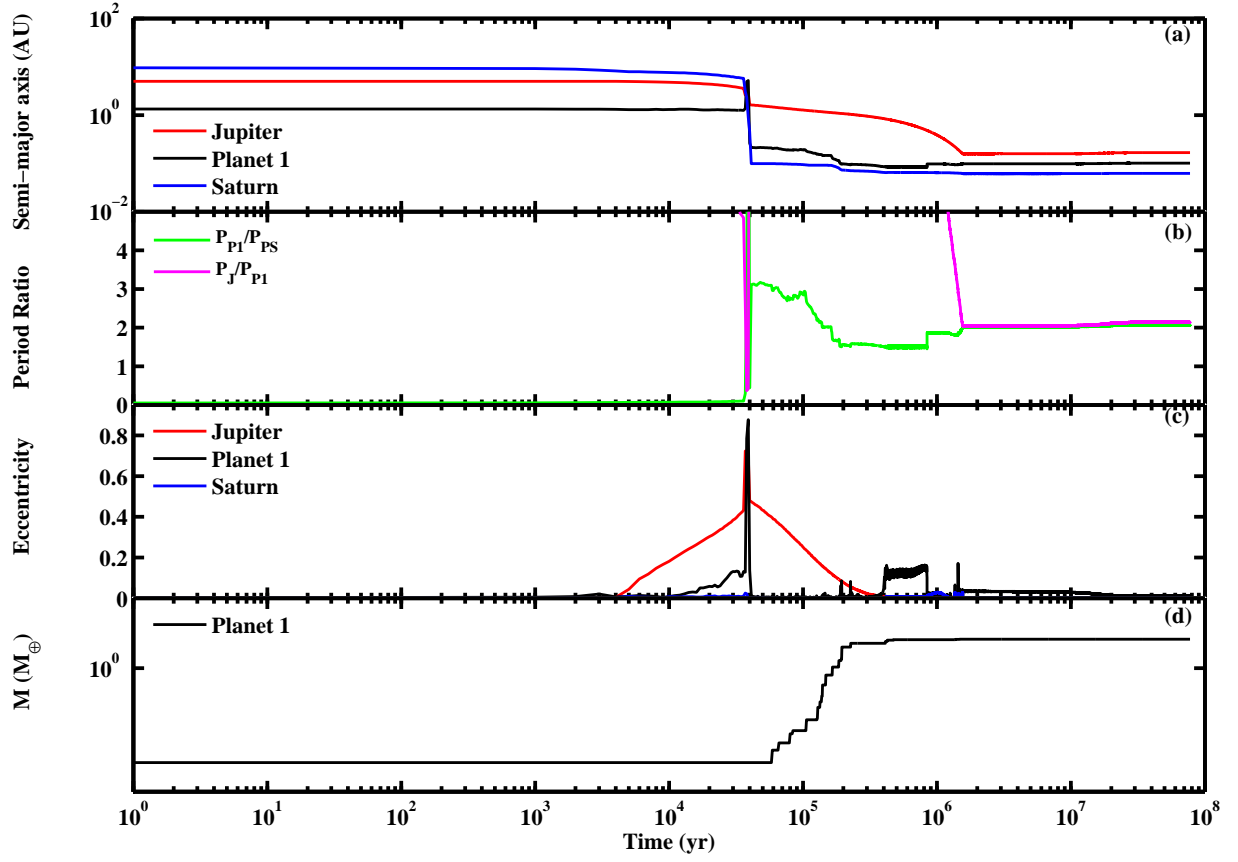


**Figure 6.** Results of the evolution of semi-major axis (upper panel) and eccentricities (lower panel) for simulation S4. One inner planet undergo type I migration while the outer two under the influence of type II migration. Note that Saturn is kicked inward and three planets are evolved into 4:2:1 MMR.

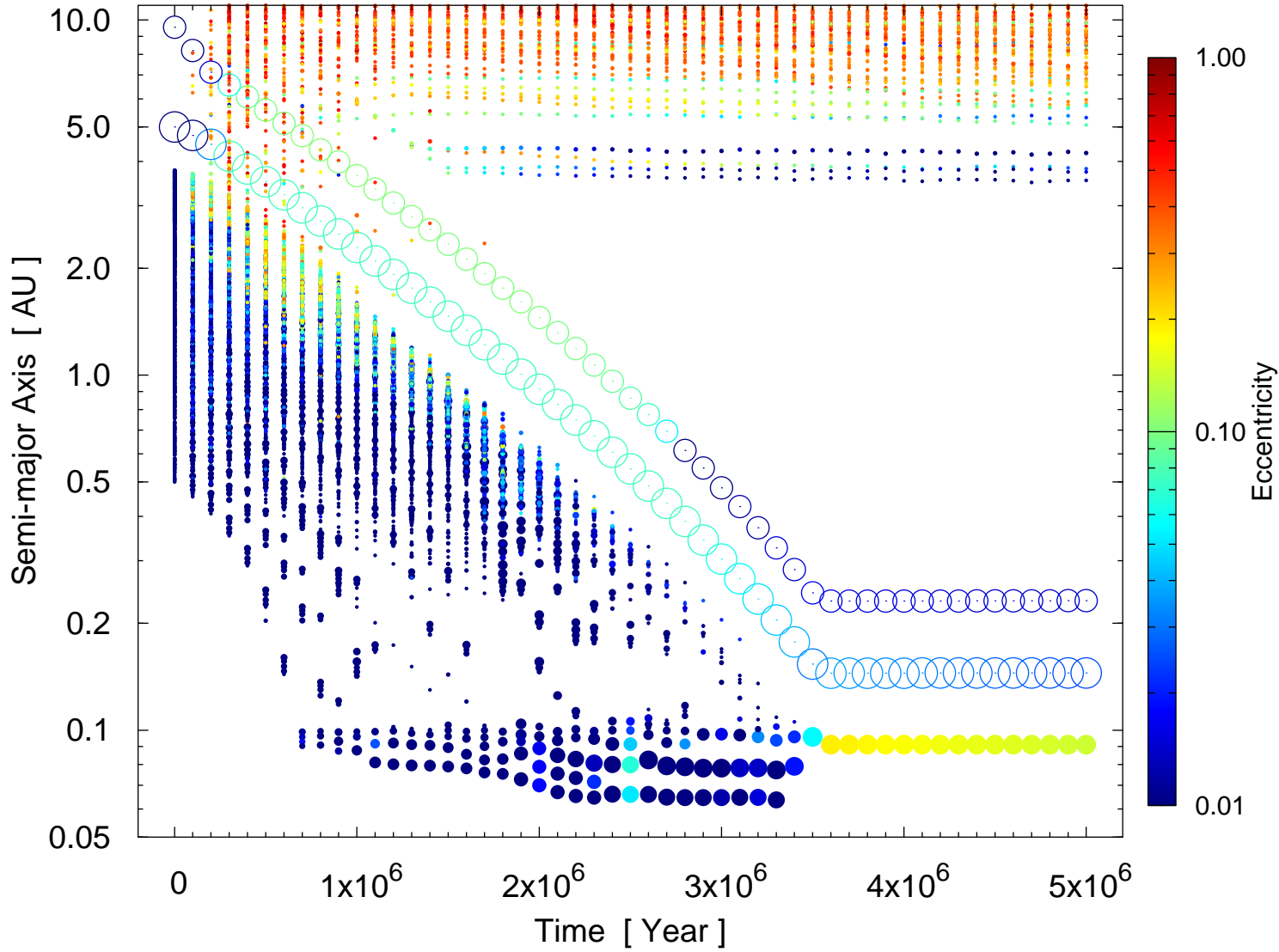


**Figure 7.** Orbital evolution of the planetesimals and two giant planets in simulation S5. The Jupiter and Saturn in this simulation underwent type II migration. The radii of the planetesimals are proportional to their mass. The color of each point shows the orbital eccentricity. Note that three planets are evolved into 4:2:1 MMR.

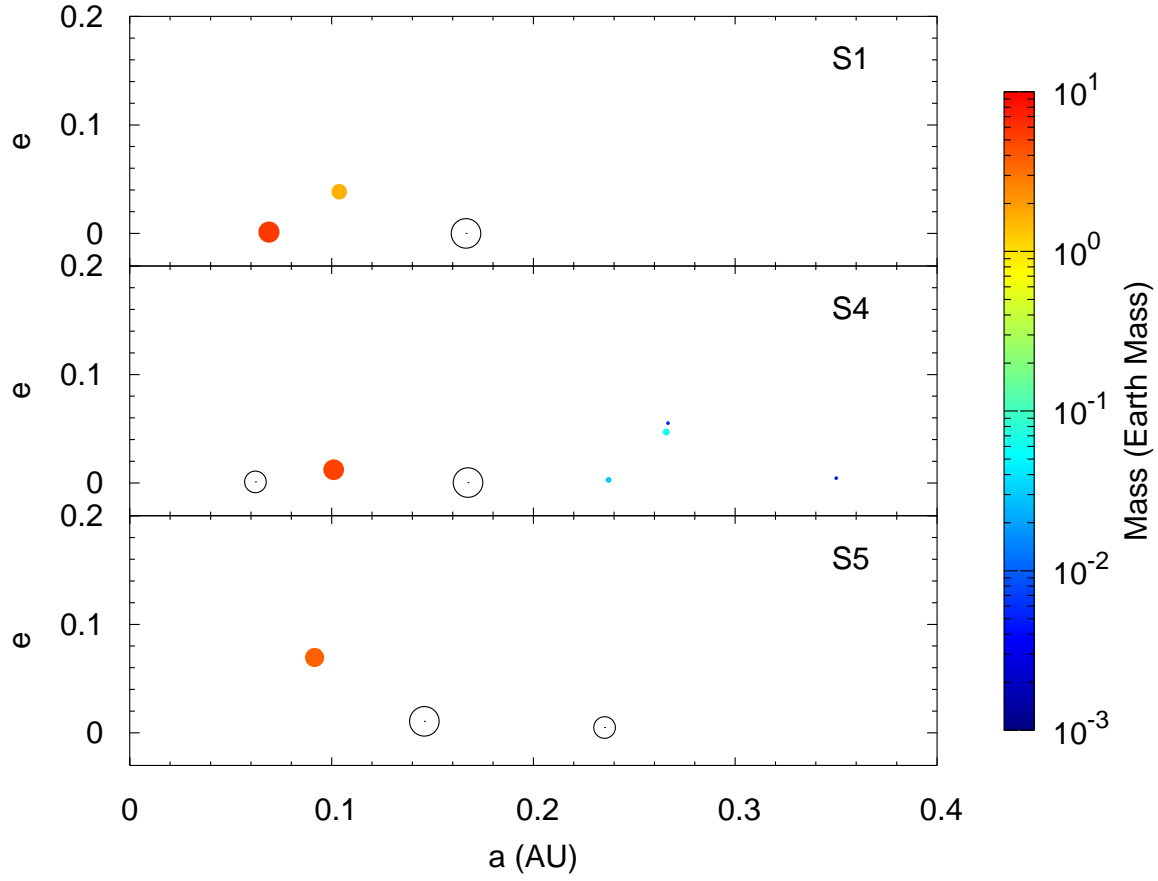


**Figure 8.** Final configuration of the 3 runs, S1, S4 and S5, that have formed 4:2:1 MMR at 100 Myr. The open circle show the giant planets. The solid point show the formed terrestrial planets. The color of the terrestrial planets show their masses.

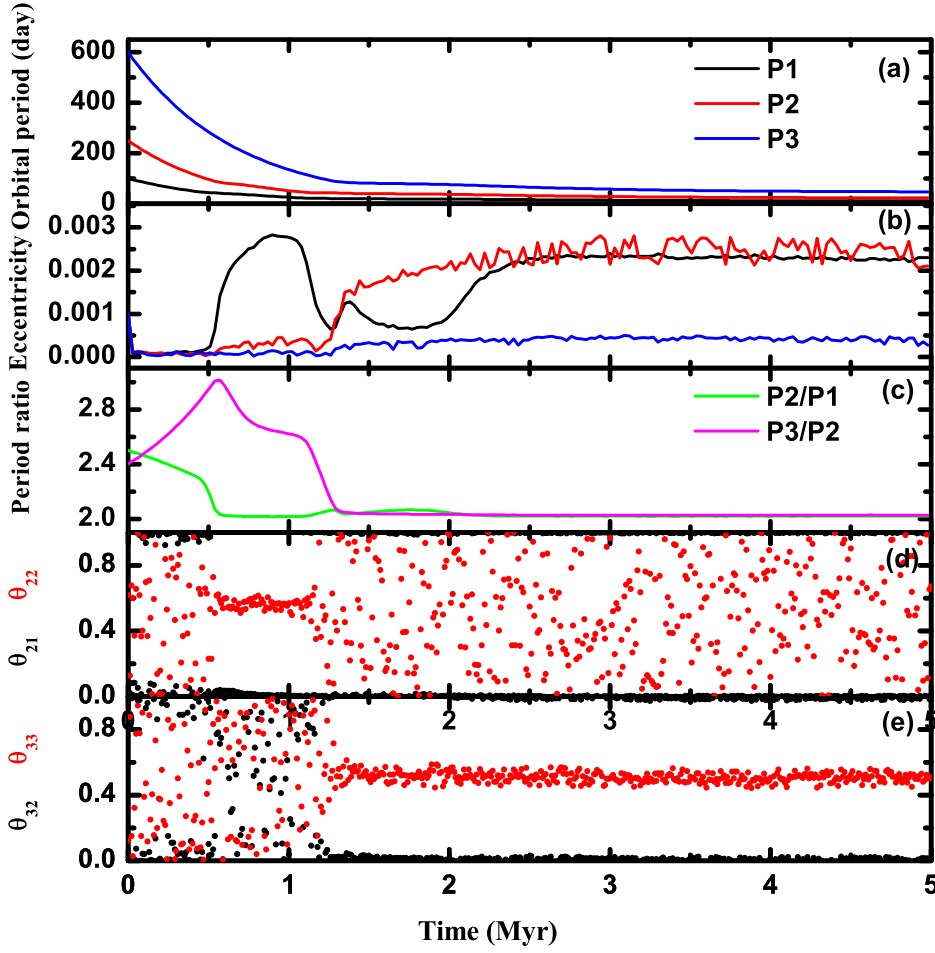


**Figure 9.** A typical run of simulations for terrestrial planets. Panel (a) shows the evolution of the orbital periods. Panel (b) displays the evolution of eccentricities and Panel (d) means the period ratio changed with the time. In panel (a) and (b), the black, red and blue lines represent the innermost (P1), middle (P2) and the outermost (P3) planets, respectively. In panel (c), the green line and pink line represent the period ratio of P2/P1 and P3/P2, respectively. Panel (d) and (e) display the resonance angles of each pairs of planets, where  $\theta_{21} = 2\lambda_1 - \lambda_2 - \varpi_1$ ,  $\theta_{22} = 2\lambda_1 - \lambda_2 - \varpi_2$ ,  $\theta_{32} = 2\lambda_2 - \lambda_3 - \varpi_2$ , and  $\theta_{33} = 2\lambda_2 - \lambda_3 - \varpi_3$ .